

Closed-form solutions of spinning, eccentric binary black holes at 1.5 post-Newtonian order

Rickmoy Samanta ¹, Sashwat Tanay ^{2,*} and Leo C. Stein ²

¹*Indian Statistical Institute, 203 B. T. Road, Kolkata 700108, India*

²*Department of Physics and Astronomy, The University of Mississippi, University, MS 38677, USA*

The closed-form solution of the 1.5 post-Newtonian (PN) accurate binary black hole (BBH) Hamiltonian system has proven to be difficult to obtain for a long time since its introduction in 1966. Closed-form solutions of the PN BBH systems with arbitrary parameters (masses, spins, eccentricity) are required for modeling the gravitational waves (GWs) emitted by them. Accurate models of GWs are crucial for their detection by LIGO/Virgo and LISA. Only recently, two solution methods for solving the BBH dynamics were proposed in Ref. [Phys. Rev. D 100, 044046 (2019)] (without using action-angle variables), and Refs. [Phys. Rev. D 103, 064066 (2021), arXiv:2110.15351] (action-angle based). This paper combines the ideas laid out in the above articles, fills the missing gaps and provides the two solutions which are fully 1.5PN accurate. We also present a public MATHEMATICA package `BBHpnToolkit` which implements these two solutions and compares them with a fully numerical treatment. The level of agreement between these solutions provides a numerical verification for all the five actions constructed in Refs. [Phys. Rev. D 103, 064066 (2021), arXiv:2110.15351]. This paper hence serves as a stepping stone for pushing the action-angle-based solution to 2PN order via canonical perturbation theory.

I. INTRODUCTION

Construction of accurate gravitational wave (GW) templates (or models) has been crucial to the hundreds of GW detections that have taken place so far since 2015 [1–3]. This is so because the method of matched filtering for GW detection requires as one of the inputs, the theoretical templates of the GW signal to be detected. Post-Newtonian (PN) theory serves as a useful framework within which GWs from binary black holes (BBHs) are modeled when the system is in its initial and longest-lived inspiral stage [4]. At this stage, the two black holes (BHs) of the BBH are far apart and move slowly around a common center. This is also referred to as the PN regime. In the PN framework, quantities of interest are presented in a PN power series in the small PN parameter (ratio of the typical speed of the system and that of light). As is typical of power series, higher-order corrections are of smaller magnitudes and carry higher PN orders. Since GWs from a BBH are functions of the positions-momenta of the source, modeling the positions-momenta of the BBH system is crucial for constructing the GW templates. This paper deals with the construction of 1.5PN accurate closed-form solutions of the BBH system.

Since we restrict ourselves to 1.5PN order, the dissipative effects on the BBH dynamics due to GW emission don't enter the picture; they show up at 2.5PN. The conservative dynamics of the system can be described with the PN Hamiltonian framework, wherein the system possesses a Hamiltonian that is a function of the system's canonical coordinates [5]. The leading PN order effect is simply that of two point masses moving under mutual Newtonian gravitational attraction whose Hamiltonian

treatment is a textbook subject matter. Such systems, move on a closed ellipse if they are bound. The next level of sophistication is at 1PN order wherein 1PN effects are added to the above Newtonian system. At this level, spin effects are ignored (they enter at 1.5PN). Ref. [6] provided the quasi-Keplerian parametric solution for this system; the trajectory was no longer a closed ellipse and the system features the advance of periastron. The orbit still remains confined in a plane due to the constancy of the angular momentum vector.

Moving further up the PN ladder, we encounter the 1.5PN system whose Hamiltonian was proposed in Ref. [7]. Via numerical integration of the resulting equations of motion (EOMs), it is seen that the orbital plane precesses; the orbital angular momentum is constant only in magnitude, but not in direction. This system displays the rich interplay of non-zero BH spins, periastron precession, along with spin and orbital-plane precession. We concern ourselves with this system in this paper.

Over the past decades, solutions to the dynamics of the spinning BBH system (at 1.5PN order or higher) have been constructed by many groups [8–16], but most of them worked under some simplifying specialization like only one BH spinning, equal masses, small eccentricity, orbit-averaging, etc. Two recent breakthroughs have happened on the front of finding solutions to the *most general* 1.5PN BBH system without any simplifying assumptions where the qualifier “most general” indicates a system with arbitrary values of masses, spins, and eccentricity, while still falling under the PN regime¹. The first breakthrough was made by Cho and Lee in Ref. [17] where they succeeded in integrating the EOMs of the system; the 1PN

* stanay@go.olemiss.edu

¹ In the PN regime, the spin angular momenta of the BHs is much smaller than the orbital angular momentum of the system.

term in the Hamiltonian was ignored throughout for simplicity. The second breakthrough came in the form of Refs. [18, 19], where the authors evaluated all the action variables (actions as in action-angle (AA) variables) and laid out a scheme on how to construct the AA-based solution of the system². Against this backdrop, this paper aims to target the following objectives

1. Re-present the solution of Ref. [17] but with the 1PN terms included. We will call it the Standard Solution.
2. Present a systematic procedure to construct the AA-based solution (as we will see later, the construction of the AA-based solution also requires input from the Standard Solution).
3. Make available `BBHpnToolkit`, a public MATHEMATICA package [21] which (1) implements the Standard Solution, the AA-based solution, and the numerical solution (2) gives the numerical values of all five frequencies (rate of increase of the angle variables) of the system (3) computes the Poisson brackets (PBs) between any two functions of the phase-space variables.

Let us mention that the AA-based solution provides a significant advantage over the Standard solution. This is so because while extending the Standard Solution to 2PN appears quite difficult, the AA-based solution should be extendable to 2PN via canonical perturbation theory. This paper assembles the ideas put forth in Refs. [18, 19, 22], and provide a solid platform from where one can springboard to push the 1.5PN solutions to 2PN order using canonical perturbation theory.

The organization of the paper is as follows. In Sec. II, we introduce the phase space, Hamiltonian, EOMs of the system as well as the concept of AA variables. In Sec. III, we re-present the solution of Ref. [22] with the 1PN terms included (Standard Solution). In Sec. IV, we lay out an in a step-by-step fashion the strategy to construct the alternative AA-based solution. In Sec. V, we introduce the MATHEMATICA package `BBHpnToolkit` that we release with this paper. We also make comparisons of our analytical solutions with the numerical one, before summarizing in Sec. VI.

II. THE SETUP

This paper is the culmination of the research initiated in Refs. [17], [18] and [19]. Since the notations and conventions used in the first article differs from those in the other two articles, the notations and conventions of this paper are a mix of the two types.

The system in consideration is a BBH system in the PN approximation. It consists of two BHs of masses m_1 and m_2 such that the relative separation from the second BH to the first one is \vec{R} . We choose to work in the center-of-mass frame throughout wherein the momenta of the first BH is equal to the negative of the other and is represented by \vec{P} . The total angular momenta of the BBH system is $\vec{J} = \vec{L} + \vec{S}_1 + \vec{S}_2$, where $\vec{L} \equiv \vec{R} \times \vec{P}$, and \vec{S}_1 and \vec{S}_2 are the spin angular momenta of the two BHs. We also define the total mass $M = m_1 + m_2$, the reduced mass $\mu \equiv m_1 m_2 / M$, the symmetric mass ratio $\nu \equiv \mu / M$, and $\sigma_1 \equiv 1 + 3m_2 / 4m_1$ and $\sigma_2 \equiv 1 + 3m_1 / 4m_2$, along with

$$\vec{S}_{\text{eff}} \equiv \sigma_1 \vec{S}_1 + \sigma_2 \vec{S}_2. \quad (1)$$

As usual, G and c denote the gravitational constant and the speed of light, respectively. Finally, note that we represent the physical time with t' , whereas $t \equiv t' / (GM)$ is reserved for the scaled time. Dots represent a derivative taken with respect to t . The norm of any 3D vector will be denoted by the same letter as the vector but without the arrow, i.e. $V \equiv |\vec{V}|$. The unit vector $\hat{V} \equiv \vec{V} / V$ corresponding to a vector \vec{V} is denoted by the use of a hat $\hat{V} \equiv \vec{V} / V$.

We now present the 1.5PN Hamiltonian of the system using scaled variables $\vec{r} \equiv \vec{R} / (GM)$, $\vec{p} \equiv \vec{P} / \mu$,

$$H = H_N + H_{1\text{PN}} + H_{1.5\text{PN}} + \mathcal{O}(c^{-4}), \quad (2)$$

where the various PN components are

$$H_N = \mu \left(\frac{p^2}{2} - \frac{1}{r} \right), \quad (3)$$

$$H_{1\text{PN}} = \frac{\mu}{c^2} \left\{ \frac{1}{8} (3\nu - 1) p^4 + \frac{1}{2r^2} \right. \quad (4)$$

$$\left. - \frac{1}{2r} [(3 + \nu)p^2 + \nu(\hat{r} \cdot \vec{p})^2] \right\}, \quad (5)$$

$$H_{1.5\text{PN}} = \frac{2G}{c^2 R^3} \vec{S}_{\text{eff}} \cdot \vec{L}. \quad (6)$$

The evolution of any function g is given by its Poisson bracket (PB) with H

$$\frac{dg}{dt'} = \{g, H\}. \quad (7)$$

A few basic rules are needed to evaluate the PB between any two functions of the phase space variables $\vec{R}, \vec{P}, \vec{S}_1$ and \vec{S}_2 , the first one being the PB between the phase space variables. The only non-vanishing PBs between the phase-space variables are given by

$$\{R^i, P_j\} = \delta_j^i, \quad \text{and} \quad \{S_a^i, S_b^j\} = \delta_{ab} \epsilon_k^{ij} S_a^k, \quad (8)$$

² See Ref. [20] for a pedagogical introduction to the action-angle method of solution.

and those related by the property of anti-symmetry of the PBs

$$\{f, g\} = -\{g, f\}. \quad (9)$$

a, b have been used to label the BHs, whereas i, j, k label the components of the vectors. The second rule is the so-called chain rule (with v_l 's standing for the phase-space variables)

$$\{f, g(v_l)\} = \{f, v_l\} \frac{\partial g}{\partial v_l}. \quad (10)$$

Finally, with the aid of Eqs. (8), (9), and (10), we can evaluate the PB between any two quantities, which facilitates the manipulation of Eq. (7) for any dynamical quantity f .

Two quantities f and g are said to commute or be in involution if $\{f, g\} = 0$. A system with Hamiltonian H in $2n$ canonical positions-momenta coordinates (\vec{Q}, \vec{P}) is said to be integrable if there exists a canonical transformation to new coordinates $(\vec{J}, \vec{\theta})$ such that all the actions \mathcal{J}^i are mutually commuting, H is a function only the \mathcal{J} 's, and that all the \vec{P} and \vec{Q} are 2π -periodic functions of the angle variables $\vec{\theta}$ [23]. An integrable system possesses n mutually commuting constants, including the Hamiltonian. Another equivalent but practically more useful definition of actions is given via [23, 24]

$$\mathcal{J}_k = \frac{1}{2\pi} \oint_{\mathcal{C}_k} \Theta = \frac{1}{2\pi} \oint_{\mathcal{C}_k} \mathcal{P}_i d\mathcal{Q}^i, \quad (11)$$

where \mathcal{C}_k is any loop in the k th homotopy class on the n -torus defined by the constant values of the n commuting constants. Before ending this section, we will touch upon the concept of flows under a function f of the phase-space variables and the associated vector fields. $f(\vec{P}, \vec{Q})$ defines a vector field as $\{\cdot, f\} = \partial/\partial\lambda$, and its action on another function $g(\vec{P}, \vec{Q})$ is $\partial g/\partial\lambda = \{g, f\}$ [25]. The integral curves of the vector field is referred to as the flow of the field. With this, it is easy to see that the equation governing the real-time evolution of a Hamiltonian system

$dg/dt' = \{g, H\}$ is basically the flow equation under the Hamiltonian where the flow parameter λ is to be taken as time t' . The next two sections deal with two equivalent ways of constructing the solution of 1.5PN BBH system.

III. THE STANDARD SOLUTION

We will construct the solution by integrating the flow equations under the 1.5PN Hamiltonian. Ref. [17] constructed the solution of the 1.5PN BBH system but with the 1PN effects excluded. Here we include the 1PN terms too. Most of the analysis in Ref. [17] goes through, even after including the 1PN terms. So, we closely follow their approach and present only the segments where the derivation presented in Ref. [17] has to be modified due to the inclusion of the 1PN terms. Ref. [17] also has some typos which we fix in this paper.

A. Angles between the \vec{L} , \vec{S}_1 and \vec{S}_2

We introduce scaled variables via $\vec{l} \equiv \vec{L}/(\mu GM)$, $h \equiv H/\mu$, and $\vec{s}_a \equiv \vec{S}_a/(\mu GM)$, where $a = 1, 2$ serve to distinguish the two BHs. Let κ_1, κ_2 and γ denote the angle between the vectors (\vec{L}, \vec{S}_1) , (\vec{L}, \vec{S}_2) , and (\vec{S}_1, \vec{S}_2) . Without loss of generality, we assume that $m_1 > m_2$. Under the 1.5PN Hamiltonian, L, S_1 and S_2 remain constant in time.

The solution for $\cos \kappa_1$ and its method of derivation is the same as that presented in Sec. III-A of Ref. [17] which was done without including the 1PN term in the Hamiltonian. Here we directly present that solution. It reads

$$\cos \kappa_1(t) = x_1 + (x_2 - x_1) \text{sn}^2(\Upsilon(t), \beta). \quad (12)$$

The quantities used in the above equation are defined below. x_1, x_2, x_3 are the roots of the cubic equation (in the order $x_1 < x_2 < x_3$)

$$\begin{aligned} & -2\delta_1 L S_1 (\delta_1 - \delta_2) \cos^3 \kappa_1 - \left[L^2 (\delta_1 - \delta_2)^2 + 2\delta_2 L \Sigma_2 S_2 (\delta_2 - \delta_1) + \delta_1^2 S_1^2 + 2\delta_1 \delta_2 \Sigma_1 S_1 S_2 + \delta_2^2 S_2^2 \right] \cos^2 \kappa_1 \\ & + 2\delta_2 S_2 [L \Sigma_1 (\delta_2 - \delta_1) + \Sigma_2 (\delta_1 S_1 + \delta_2 \Sigma_1 S_2)] \cos \kappa_1 - \delta_2^2 S_2^2 (\Sigma_1^2 + \Sigma_2^2 - 1) = 0. \end{aligned} \quad (13)$$

Σ_1, Σ_2 and $\delta_{1/2}$ are defined as

$$\Sigma_1 \equiv \frac{\vec{S}_1 \cdot \vec{S}_2}{S_1 S_2} - \frac{L}{S_2} \frac{\delta_1 - \delta_2}{\delta_2} \frac{\vec{L} \cdot \vec{S}_1}{L S_1}, \quad (14)$$

$$\Sigma_2 \equiv \frac{\vec{L} \cdot \vec{S}_2}{L S_2} + \frac{\delta_1 S_1}{\delta_2 S_2} \frac{\vec{L} \cdot \vec{S}_1}{L S_1}, \quad (15)$$

$$\delta_a \equiv 2 \frac{m_1 m_2}{M^2} \sigma_a, \quad (a = 1, 2). \quad (16)$$

We need more definitions to fully explicate the solution given in Eq. (12).

$$\Upsilon(t) = \frac{\sqrt{A(x_3 - x_1)}}{2} \left(\alpha + \frac{v + e \sin v}{c^2 l^3} \right), \quad (17)$$

$$\beta = \sqrt{\frac{x_2 - x_1}{x_3 - x_1}}, \quad (18)$$

$$\alpha = \frac{\pm 2}{\sqrt{A(x_3 - x_1)}} F\left(\arcsin \sqrt{\frac{\cos \kappa_1(t=0) - x_1}{x_2 - x_1}}, \beta\right), \quad (19)$$

$$A = 2ls_1\delta_1(\delta_2 - \delta_1), \quad (20)$$

$$v = 2 \arctan\left(\sqrt{\frac{1+e}{1-e}} \tan \frac{u}{2}\right), \quad \text{or} \quad (21)$$

$$= u + 2 \arctan\left(\frac{\beta_e \sin u}{1 - \beta_e \cos u}\right), \quad (22)$$

$$\beta_e = \frac{e}{1 + (1 - e^2)^{1/2}}, \quad (23)$$

$$n(t - t_0) = u - e \sin u, \quad (24)$$

$$n = (-2h)^{3/2}, \quad (25)$$

$$e = \sqrt{1 + 2hl^2}, \quad (26)$$

$$F(\phi_p, k) \equiv \int_0^{\phi_p} \frac{d\theta}{\sqrt{1 - k^2 \sin^2 \theta}}, \quad (27)$$

$$\text{sn}(F, k) \equiv \sin(\text{am}(F, k)) \equiv \sin \phi_p. \quad (28)$$

Note that Eqs. (21), (24), (25), and (26) give the true anomaly, Kepler equation, mean motion and the eccentricity, respectively, all at the Newtonian level. Note that Eq. (22) is preferred over Eq. (21) because its RHS does not have the discontinuity features due to arctan, the way the RHS of Eq. (21) has. In Eqs. (27) and (28), F is the incomplete elliptic integral of the first kind, whereas sn and am are the Jacobi sin and amplitude functions respectively. Finally, the + sign in Eq. (19) is chosen if

$d \cos \kappa_1 / dt > 0$ at initial time, otherwise we choose the – sign.

The cosine of the other two angles κ_2 and γ between the angular momenta can be easily had from the solution for $\cos \kappa_1$ as given in Eq. (12), and supplemented by Eqs. (14) and (15) which when written in a slightly different form read

$$\cos \gamma = \Sigma_1 + \frac{L}{S_2} \frac{\delta_1 - \delta_2}{\delta_2} \cos \kappa_1, \quad (29)$$

$$\cos \kappa_2 = \Sigma_2 - \frac{\delta_1 S_1}{\delta_2 S_2} \cos \kappa_1. \quad (30)$$

B. Solution for \vec{L}

For the solution of \vec{L} , we will use an inertial frame (call it IF), whose z -axis is aligned with \vec{J} . In this frame, \vec{L} has a polar angle θ_L and an azimuthal angle ϕ_L . Because $dL/dt = 0$, we need to determine only these two angles to determine \vec{L} . Since

$$\cos \theta_L = \frac{\vec{L} \cdot \vec{J}}{LJ} = \frac{L^2 + LS_1 \cos \kappa_1 + LS_2 \cos \kappa_2}{LJ}, \quad (31)$$

this means that we can construct $\cos \theta_L$ as a function of time from our already-constructed solutions for the cosines of κ_1, κ_2 and γ in Sec. III A.

The solution for the azimuthal angle ϕ_L of \vec{L} in IF and its method of derivation closely follows Sec. III-B of Ref. [17]. So we again directly present the solution here which reads

$$\phi_L(t) - \phi_{L_0} = \mathcal{F}(t), \quad (32)$$

where the function $\mathcal{F}(t)$ is

$$\mathcal{F}(t) = \frac{2}{\sqrt{A(x_3 - x_1)}} \left(\frac{\beta_1 \Pi\left(\frac{x_1 - x_2}{\alpha_1 + x_1}, \text{am}(\Upsilon, \beta), \beta\right)}{\alpha_1 + x_1} - \frac{\beta_2 \Pi\left(\frac{x_1 - x_2}{\alpha_2 + x_1}, \text{am}(\Upsilon, \beta), \beta\right)}{\alpha_2 + x_1} \right), \quad (33)$$

where

$$\alpha_1 = -\frac{\delta_2(j + l + s_2\sigma_2)}{s_1(\delta_1 - \delta_2)} \quad (34)$$

$$\alpha_2 = -\frac{\delta_2(-j + l + s_2\sigma_2)}{s_1(\delta_1 - \delta_2)} \quad (35)$$

$$\beta_1 = -\delta_2 \frac{l^2\delta_1 + j^2\delta_2 + s_1(\delta_1 - \delta_2)(s_1 + s_2\sigma_1) + ls_2\delta_1\sigma_2 + j[l(\delta_1 + \delta_2) + s_2\sigma_2\delta_2]}{2s_1(\delta_1 - \delta_2)}, \quad (36)$$

$$\beta_2 = -\delta_2 \frac{l^2\delta_1 + j^2\delta_2 + s_1(\delta_1 - \delta_2)(s_1 + s_2\sigma_1) + ls_2\delta_1\sigma_2 - j[l(\delta_1 + \delta_2) + s_2\sigma_2\delta_2]}{2s_1(\delta_1 - \delta_2)}. \quad (37)$$

ϕ_{L_0} is an integration constant to be determined by substituting $t = 0$ in Eq. (32). Note that the corresponding equations in Ref. [17] (Eqs. (3.28)) have typos.

C. Solution for \vec{S}_1 and \vec{S}_2

In Ref. [17], the full solution of \vec{S}_1 was not presented in the same way as for \vec{L} . However, the method of constructing the solution for \vec{S}_1 parallels very closely that of constructing the \vec{L} vector solution³. So, again we merely present the solution without derivation.

Just like \vec{L} , \vec{S}_1 is described by its polar and azimuthal angles (θ_{S_1} and ϕ_{S_1} respectively) because its magnitude

is fixed. For the polar angle, we have just like before

$$\begin{aligned} \cos \theta_{S_1} &= \frac{\vec{S}_1 \cdot \vec{J}}{S_1 J} = \frac{S_1^2 + \vec{L} \cdot \vec{S}_1 + \vec{S}_1 \cdot \vec{S}_2}{S_1 J} \\ &= \frac{S_1^2 + L S_1 \cos \kappa_1 + S_1 S_2 \cos \gamma}{S_1 J}, \end{aligned} \quad (38)$$

which means that $\cos \theta_{S_1}$ can be had from our previously constructed solutions of cosines of κ_1, κ_2 and γ .

The solution for the azimuthal angle $\phi_{S_1}(t)$ of \vec{S}_1 in IF is given by

$$\phi_{S_1}(t) - \phi_{S_{10}} = \mathcal{G}(t), \quad (39)$$

where the function $\mathcal{G}(t)$ is

$$\mathcal{G}(t) = \frac{2}{\sqrt{A(x_3 - x_1)}} \left(\frac{\beta_{1s1} \Pi \left(\frac{x_1 - x_2}{\alpha_{1s1} + x_1}, \text{am}(\Upsilon, \beta), \beta \right)}{\alpha_{1s1} + x_1} - \frac{\beta_{2s1} \Pi \left(\frac{x_1 - x_2}{\alpha_{2s1} + x_1}, \text{am}(\Upsilon, \beta), \beta \right)}{\alpha_{2s1} + x_1} \right) + \frac{v + e \sin v}{c^2 l^3} j \delta_2, \quad (40)$$

with

$$\alpha_{1s1} = \frac{\delta_2 (-j + s_1 + s_2 \sigma_1)}{l \delta_1}, \quad (41)$$

$$\alpha_{2s1} = \frac{\delta_2 (j + s_1 + s_2 \sigma_1)}{l \delta_1}, \quad (42)$$

$$\beta_{1s1} = -\delta_2 \frac{l^2 \delta_1 + (s_1 (\delta_1 - \delta_2) + j \delta_2) (-j + s_1 + s_2 \sigma_1) + l s_2 \delta_1 \sigma_2}{2l \delta_1}, \quad (43)$$

$$\beta_{2s1} = \delta_2 \frac{-l^2 \delta_1 + (-s_1 \delta_1 + (j + s_1) \delta_2) (j + s_1 + s_2 \sigma_1) - l s_2 \delta_1 \sigma_2}{2l \delta_1}. \quad (44)$$

$\phi_{S_{10}}$ is an integration constant to be determined by substituting $t = 0$ in Eq. (39). This completes the solution for \vec{S}_1 . Now \vec{S}_2 can also be easily had from

$$\vec{S}_2 = \vec{J} - \vec{L} - \vec{S}_1. \quad (45)$$

D. Solution for \vec{R}

The solution for \vec{R} proceeds along the same lines as in Ref. [17], but is modified somewhat due to the inclusion of the 1PN term in the Hamiltonian. So, unlike previous sub-sections, we will present the derivation of the phase of \vec{R} before presenting its solution. The magnitude of \vec{R}

has already been worked out in the literature, so we won't present its derivation.

Specification of $\vec{r} = \vec{R}/(GM)$ requires specifying its magnitude and direction. The magnitude has been worked out in the past. The 1PN and 2PN contributions (without spins) can be found in Ref. [6], whereas the 1.5PN contribution (with the 1PN effects ignored) can be found in Ref. [26]. Combining these results together, we have up to 1.5PN order the following quasi-Keplerian parametric solution for r

$$\begin{aligned} r &= a_r (1 - e_r \cos u), \\ l &\equiv n (t - t_0) = u - e_t \sin u, \end{aligned} \quad (46)$$

with u and l standing for the eccentric and the mean anomalies, respectively. The other constants that com-

³ \vec{L} solution was constructed in Ref. [17] by introducing an " \vec{L} -centered" non-inertial frame, whose z -axis was aligned with \vec{L} . To construct the \vec{S}_1 solution using this method, we need to introduce an " \vec{S}_1 -centered" non-inertial frame whose z -axis is aligned with \vec{S}_1 .

prise the above solution are

$$a_r = -\frac{1}{2h} \left(1 - \frac{1}{2}(\nu - 7)\frac{h}{c^2} - 2\frac{s_{\text{eff}} \cdot l}{l^2} \frac{h}{c^2} \right), \quad (47)$$

$$e_r^2 = 1 + 2hl^2 - 2(6 - \nu)\frac{h}{c^2} - 5(3 - \nu)\frac{h^2 l^2}{c^2} + 8(1 + hl^2)\frac{s_{\text{eff}} \cdot l}{l^2} \frac{h}{c^2}, \quad (48)$$

$$n = (-2h)^{3/2} \left(1 + \frac{2h}{8c^2}(\nu - 15) \right), \quad (49)$$

$$e_t^2 = 1 + 2hl^2 + 4(1 - \nu)\frac{h}{c^2} + (17 - 7\nu)\frac{h^2 l^2}{c^2} + 4\frac{s_{\text{eff}} \cdot l}{l^2} \frac{h}{c^2}, \quad (50)$$

where the following definitions have been used

$$\vec{s}_{\text{eff}} \equiv \delta_1 \vec{s}_1 + \delta_2 \vec{s}_2, \quad (51)$$

$$s_{\text{eff}} \cdot l \equiv \vec{s}_{\text{eff}} \cdot \vec{l}. \quad (52)$$

This definition implies the following relation

$$\vec{s}_{\text{eff}} \equiv \frac{2\nu}{\mu GM} \vec{S}_{\text{eff}}. \quad (53)$$

With the magnitude of \vec{r} being taken care of, now we can move on to determine its phase in a plane perpendicular to \vec{l} . The scaled-time derivative of the scaled position vector \vec{r} is

$$\begin{aligned} \frac{d\vec{r}}{dt} &= \{\vec{r}, H\} \\ &= \vec{p} + \frac{1}{2c^2 r^3} (-2\nu(\vec{p} \cdot \vec{r})\vec{r} - (6 + 2\nu)r^2 \vec{p} \\ &\quad + (3\nu - 1)p^2 r^3 \vec{p} - 2\vec{r} \times \vec{s}_{\text{eff}}), \end{aligned} \quad (54)$$

which when solved perturbatively gives the following expression for \vec{p}

$$\begin{aligned} \vec{p} &= \frac{d\vec{r}}{dt} \\ &+ \frac{1}{c^2} \left(\frac{\vec{r} \times \vec{s}_{\text{eff}} + \nu(\vec{p} \cdot \vec{r})\vec{r}}{r^3} + \frac{d\vec{r}}{dt} \left(\frac{p^2}{2} - \frac{3p^2 \nu}{2} + \frac{3 + \nu}{r} \right) \right) \end{aligned} \quad (56)$$

At this point, we introduce a non-inertial frame (call it NIF) whose x, y and z axes are along $\vec{J} \times \vec{L}$, $\vec{L} \times (\vec{J} \times \vec{L})$ and \vec{L} , respectively. The Euler matrix which when multiplied with a column consisting of a vector's components in IF gives its components in NIF is

$$E_L = \begin{pmatrix} -\sin \phi_L & \cos \phi_L & 0 \\ -\cos \theta_L \cos \phi_L & -\cos \theta_L \sin \phi_L & \sin \theta_L \\ \cos \phi_L \sin \theta_L & \sin \theta_L \sin \phi_L & \cos \theta_L \end{pmatrix} \quad (57)$$

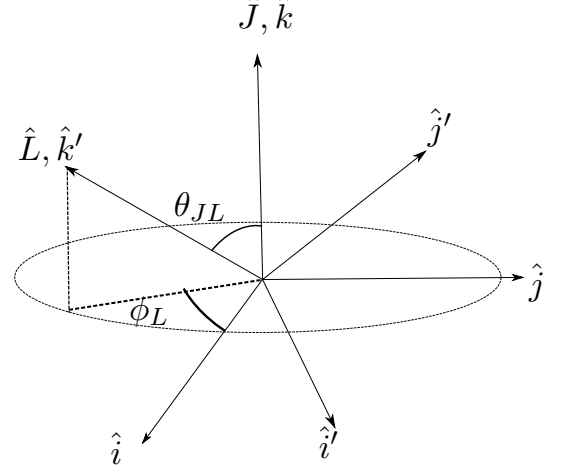


FIG. 1: The non-inertial ($i'j'k'$) frame (centered around $\hat{L} \equiv \vec{L}/L$) is displayed along with the inertial (ijk) frame (centered around $\hat{J} \equiv \vec{J}/J$).

In NIF, various vector components are

$$\vec{l} = \begin{bmatrix} 0 \\ 0 \\ l \end{bmatrix}_n \quad (58)$$

$$\vec{s}_1 = s_1 \begin{bmatrix} \sin \kappa_1 \cos \xi \\ \sin \kappa_1 \sin \xi \\ \cos \kappa_1 \end{bmatrix}_n \quad (59)$$

$$\vec{s}_2 = s_2 \begin{bmatrix} \sin \kappa_2 \cos (\xi + \psi) \\ \sin \kappa_2 \sin (\xi + \psi) \\ \cos \kappa_2 \end{bmatrix}_n \quad (60)$$

$$\vec{r} = \begin{bmatrix} r \cos \phi \\ r \sin \phi \\ 0 \end{bmatrix}_n \quad (61)$$

Note that with the aid of Eqs. (59) and (60), we have actually defined the angles ξ and ψ , that is to say, ξ and $\xi + \psi$ are azimuthal angles of \vec{s}_1 and \vec{s}_2 in NIF. Implicit in Eq. (61) is the definition that ϕ is the azimuthal angle of \vec{r} in NIF. Also, the subscript “ n ” after the above column vectors denotes that the components have been written in NIF.

Being cognizant of the fact that the time derivative of a vector changes (as a geometrical object) with a change of the frame in which it is viewed (see Sec. 4.9 of Ref. [27]), we mention here that all time derivatives of vectors in this paper are to be viewed in IF. With that, we now wish to express the components of $d\vec{r}/dt$ in NIF. We do so by first

writing the \vec{r} -components in IF (using Eqs. (57) and (61)), taking derivatives of the components with respect to t , and then writing the components of the time derivative

in NIF (using E_L^{-1}). The end result is

$$\dot{\vec{r}} = \begin{bmatrix} \dot{r} \cos \phi - r \sin \phi (\dot{\phi}_L \cos \theta_L + \dot{\phi}) \\ \dot{r} \sin \phi + r \cos \phi (\dot{\phi}_L \cos \theta_L + \dot{\phi}) \\ r (-\dot{\phi}_L \sin \theta_L \cos \phi + \dot{\theta}_L \sin \phi) \end{bmatrix}_n \quad (62)$$

Now using Eqs. (56)-(62), we express $\vec{l} = \vec{r} \times \vec{p}$ in NIF, and its third component when written out gives us (with $\epsilon \equiv 1/c^2$ and $h \equiv H/\mu$)

$$\frac{d\phi}{dt} = -\frac{2(\epsilon s_1 \delta_1 \cos \kappa_1 + \epsilon s_2 \delta_2 \cos \kappa_2 + lr)}{r^2 (-2\epsilon(3 + \nu) + (-2 + \epsilon(-1 + 3\nu))((\vec{p} \cdot \hat{r})^2 + \frac{l^2}{r^2}))r} - \cos \theta_L \frac{d\phi_L}{dt}, \quad (63)$$

In the above equation, p^2 was eliminated with the aid of

$$p^2 = (\vec{p} \cdot \hat{r})^2 + \frac{l^2}{r^2}. \quad (64)$$

We also re-present Eq. (36) of Ref. [18]

$$\vec{p} \cdot \hat{r} = \left((2h - \epsilon(3\nu - 1)h^2) + \frac{2(1 + \epsilon(4 - \nu)h)}{r} + \frac{(-l^2 + \epsilon(6 + \nu))}{r^2} + \frac{-\epsilon\nu(l^2 + 2s_{\text{eff}} \cdot l/\nu)}{r^3} \right)^{1/2}. \quad (65)$$

We also have

$$\vec{L} \cdot \vec{J} = JL \cos \theta_L = L^2 + LS_1 \cos \kappa_1 + LS_2 \cos \kappa_2, \quad (66)$$

$$\frac{d\phi_L}{dt} = \frac{1}{c^2 r^3} \left(\frac{\beta_1}{\cos \kappa_1 + \alpha_1} - \frac{\beta_2}{\cos \kappa_1 + \alpha_2} \right). \quad (67)$$

Eq. (67) has already been derived in Ref. [17], see its Eq. (3.27).

Making use of Eqs. (65), (66), (67), (29) and (30), we can rewrite Eq. (63) in terms of $\cos \kappa_1$

$$\begin{aligned} \frac{d\phi}{dt} &= \frac{\epsilon}{r^3} \left(\frac{\beta_1}{\cos \kappa_1 + \alpha_1} + \frac{\beta_2}{\cos \kappa_1 + \alpha_2} \right) \\ &\quad - \frac{l\epsilon^2(-1 + 3\nu)(2s_{\text{eff}} \cdot l + l^2\nu)}{2r^5} + \frac{l\epsilon^2(-6 + 17\nu + 3\nu^2)}{2r^4} + \frac{l(2 - h^2\epsilon^2(1 - 3\nu)^2 + 2h\epsilon(-1 + 3\nu))}{2r^2} \\ &\quad - \frac{\epsilon(-s_{\text{eff}} \cdot l + l^2(4 + 4h\epsilon - 2\nu - 13h\epsilon\nu + 3h\epsilon\nu^2 + \delta_1 + \delta_2) + ls_2\delta_2\Sigma_2)}{lr^3}, \end{aligned} \quad (68)$$

$$\equiv \frac{\epsilon}{r^3} \left(\frac{\beta_1}{\cos \kappa_1 + \alpha_1} + \frac{\beta_2}{\cos \kappa_1 + \alpha_2} \right) + \frac{A_5}{r^5} + \frac{A_4}{r^4} + \frac{A_3}{r^3} + \frac{A_2}{r^2}. \quad (69)$$

which when integrated gives

$$\phi - \phi_0 = \frac{2}{\sqrt{A(x_3 - x_1)}} \left(\frac{\beta_1 \Pi\left(\frac{x_1 - x_2}{\alpha_1 + x_1}, \text{am}(\Upsilon, \beta), \beta\right)}{\alpha_1 + x_1} + \frac{\beta_2 \Pi\left(\frac{x_1 - x_2}{\alpha_2 + x_1}, \text{am}(\Upsilon, \beta), \beta\right)}{\alpha_2 + x_1} \right) + A_5 \mathcal{R}_5 + A_4 \mathcal{R}_4 + A_3 \mathcal{R}_3 + A_2 \mathcal{R}_2, \quad (70)$$

where ϕ_0 is an integration constant to be determined by substituting $t = 0$ in the above equation. Also, \mathcal{R}_j is the indefinite integral of r^{-j} with respect to t . For brevity, we don't write out \mathcal{R}_j 's but they can be easily had from

the Newtonian-accurate expressions

$$r = a(1 - e \cos u), \quad (71)$$

$$l \equiv n(t - t_0) = u - e \sin u. \quad (72)$$

n and e are given in Eqs. (26) and (25), respectively. a is the Newtonian version of the RHS of Eq. (47). Note that we have kept more than necessary PN accuracy in Eq. (68) and by extension, Eq. (70) just for the purposes of illustration; any additive term containing ϵ^q with $q \geq 2$ can be dropped.

E. Solution for \vec{P}

We present the determination of $\vec{P} = \mu\vec{p}$ in a step-by-step algorithmic fashion

1. From Eqs. (64) and (65), determine p^2 or p . What now remains is to determine the azimuthal angle of \vec{p} in NIF.
2. Determine

$$\phi_{\text{temp-offset}} \equiv \arcsin \frac{L(t)}{r(t)p(t)}. \quad (73)$$

3. The azimuthal angle that \vec{p} makes with the x -axis of NIF is $\phi + \phi_{\text{offset}}$, where

$$\begin{aligned} \phi_{\text{offset}} &= \phi_{\text{temp-offset}} & \text{if } \vec{p} \cdot \hat{r} > 0, \\ \phi_{\text{offset}} &= \pi - \phi_{\text{temp-offset}} & \text{if } \vec{p} \cdot \hat{r} < 0. \end{aligned} \quad (74)$$

IV. ACTION-ANGLE BASED SOLUTION

We devote this section to explaining our construction of an alternate AA-based solution to the 1.5PN BBH system. We will present in a step-by-step algorithmic fashion.

1. The 1.5PN system has five commuting constants $\vec{C} = \{J, J_z, L, H, S_{\text{eff}} \cdot L\}$ and five action variables $\vec{\mathcal{J}} = \{\mathcal{J}_1 = J, \mathcal{J}_2 = J_z, \mathcal{J}_3 = L, \mathcal{J}_4, \mathcal{J}_5\}$, which can be found in Refs. [18] and [19]; their notations and definitions are somewhat different from those in this paper.

2. Under the real-time evolution of the BBH system, the angles change as $\Delta\theta_i = \omega_i t'$, $t' = tGM$ being the physical time; ω_i 's are naturally called the frequencies of the system and are constants, for they functions of the constant action variables. Sec. VI-A of Ref. [19] shows how to compute the five frequencies. The process mainly consists of constructing the Jacobian matrix of the actions with respect to the commuting constants, inverting this Jacobian matrix, and the row corresponding to the Hamiltonian (one of the commuting constants) consists of the five frequencies.

3. Let all the phase space variables be collectively denoted by $\vec{V} = \{\vec{R}, \vec{P}, \vec{S}_1, \vec{S}_2\}$ with their initial values being $\vec{V}_0 \equiv \vec{V}(t' = 0)$. Suppose the state of the system is given at $t' = 0$ in the form of \vec{V}_0 , and we are required to compute $\vec{V}(t')$ at any non-zero time t' .

4. At $t' = 0$, assign all the angle variables of the system to have the value equal to 0; $\vec{\theta}(t' = 0) = \vec{0}$. Then at

the final time t' , the angles of the system would have become $\vec{\theta} = \vec{\omega} \times t'$. The problem of finding the state of the system at t' now becomes that of increasing all the angle variables by $\vec{\omega} \times t'$.

5. As shown in Sec VI-B of Ref. [19], the angle θ_i can be increased by a certain amount if we flow under the corresponding action \mathcal{J}_i by the same amount. Therefore the problem becomes that of flowing under the actions \mathcal{J}_i by amounts $\omega_i t'$ (starting from the \vec{V}_0 configuration). The order of flows does not matter because just like all the members of \vec{C} , all the actions mutually commute among themselves too.

6. Because the flow equation under the actions reads

$$\frac{d\vec{V}}{d\lambda} = \left\{ \vec{V}, \mathcal{J}_i(\vec{C}) \right\} = \left\{ \vec{V}, C_j \right\} \frac{\partial \mathcal{J}_i}{\partial C_j}, \quad (75)$$

it means that a flow under an action \mathcal{J}_i by $\Delta\lambda_i$ can be achieved by flowing under all the commuting constants C_j 's by respective amounts $(\partial \mathcal{J}_i / \partial C_j) \Delta\lambda_i$. Again, we can flow under the commuting constants C_j 's in any order, since they all mutually commute. This finally breaks down our problem to that of flowing under all five C_j 's by certain amounts, whose closed-form solution is discussed below.

Now it should be clear as to why the AA-based solution relies on the Standard Solution presented in Sec. III. This is so because one of the commuting constants is the Hamiltonian and in Sec. III, we presented the solution of the flow under this commuting constant. Nevertheless, the AA-based solutions appears to the superior one in that there is hope to push it to 2PN using canonical perturbation theory which is a perturbation technique designed around the action-angle framework [27].

V. SOFTWARE PACKAGE AND COMPARISON OF THE SOLUTIONS

With this article, we are releasing a public MATHEMATICA package `BBHpnToolkit`, which accomplishes the following objectives [21].

1. Implements the Standard Solution of Sec. III got by integrating the flow under the Hamiltonian.
2. Implements the action-angle-based solution of Sec. IV.
3. Gives the numerical solution of the system
4. Gives the numerical values of all five frequencies of the system, wherein by frequency we refer to the rate of increase of the five angles (as in action-angle variables) of the system.

For the reference of the future users of our MATHEMATICA package, we mention herein that we have retained some unnecessary high PN terms in the coded expressions which implement the two analytical solutions in the package.

The full account is given in Appendix B. We devote this section to investigating the PN accuracy of the two analytical solutions with respect to the one got by direct numerical integration of the EOMs. In this section, we will refer to both these two analytical solutions collectively as just “analytical solutions”, for these two analytical solutions overlap with each other much better than they do with the numerical one.

We first begin by displaying the plots of the analytical solutions along with the numerical one in Fig. 2. Plots corresponding to the two analytical solutions (Standard and AA-based solutions) cannot be distinguished visually. But they are collectively distinguishable from the numerical solution at late times. As displayed in the caption of this figure, the parameters taken for these plots do not correspond to astrophysically relevant systems. But this is not a cause of concern because our focus in this section is to explore the mathematical accuracy of our solutions which are valid for a wide set of parameters, and not just those which correspond to real astrophysical scenarios. Later in this section, we will see that it is actually helpful to study these solutions under non-physical scenarios (such as changing the value of $\epsilon \equiv 1/c^2$), to determine the PN accuracy of our solutions (via the method of linear fit between the error and the PN parameter).

Let us now switch to a more technical task of determining the PN accuracy of our analytical solutions against the numerical one (one got by numerical integration of the EOMs). We explain our comparison method with the aid of Fig. 3. Starting from $t = t_0 = 0$, we evolve the system numerically up to a certain time $t = t_1$, such that \vec{R}_n (\vec{R} got via numerical integration) differs by a small amount from \vec{R}_a (\vec{R} got from the analytical solution). By “small amount”, we mean an opening angle (ζ_3 in Fig. 3) of $\sim 0.5^\circ$ to 1° between \vec{R}_a and \vec{R}_n . The dashed circle in the figure denotes the plane perpendicular to \vec{L}_n (\vec{L} got via numerical integration at $t = t_1$). $\vec{R}_{a\parallel}$ is the projection of \vec{R}_a on this plane. We mention that the difference between \vec{R}_n and \vec{R}_a is greatly exaggerated in this figure for the purposes of illustration. Now, even if we ignore the numerical roundoff errors, we expect $\vec{R}_a \neq \vec{R}_n$ because of the PN truncation errors that crept in while deriving the analytical solutions. For this section, we force the roundoff errors to be much smaller than the truncation errors by keeping sufficient numerical precision while constructing the numerical solution.

Now, the $\vec{R}_a - \vec{R}_n$ can be broken down into two components: an in-plane component $\vec{R}_{a\parallel} - \vec{R}_n$, and an out-of-plane component $\vec{R}_a - \vec{R}_{a\parallel}$. The in-plane difference is brought about by an in-plane (perpendicular to \vec{L}) dephasing which occurs due to the difference between the numerical and the analytical values of the mean motion n (a kind of frequency). The out-of-plane difference is brought about by the difference $\vec{L}_a - \vec{L}_n$, where \vec{L}_a is the analytical \vec{L} .

For comparison purposes, it is convenient to think of the in-plane and out-of-plane differences as in-plane and out-of-plane dephasings happening due to a difference in some angular velocities $d\omega_{\parallel}$, and $d\omega_{\perp}$ in the two directions, with the former being essentially the difference between the analytical and numerical mean motions. As is suggested from Eq. (49), these frequencies are often expressible as a PN series. Hence, we schematically write the difference between the numerical and analytical frequencies as a PN series along the two directions as

$$d\omega_{\parallel} = \xi^p d\omega_{\parallel p} + \xi^{p+1} d\omega_{\parallel p+1} + \mathcal{O}(\xi^{p+2}), \quad (76)$$

$$d\omega_{\perp} = \xi^q d\omega_{\perp q} + \xi^{q+1} d\omega_{\perp q+1} + \mathcal{O}(\xi^{q+2}), \quad (77)$$

with ξ standing for the PN parameter $GM/(c^2 R)$. The above equations indicate that the differences in the frequencies along the two directions occurs at PN orders p and q . Note that unlike earlier sections, p does not stand for the magnitude of the scaled momentum, but is rather a PN power-counting index. It then follows that

$$|\vec{R}_{a\parallel} - \vec{R}_n| = \xi^p R_n d\omega_{\parallel p} t_0, \quad (78)$$

$$|\vec{R}_a - \vec{R}_{a\parallel}| = \xi^q R_n d\omega_{\perp q} t_0, \quad (79)$$

where the LHS is the small arc length which subtends an angle $\xi^p d\omega_{\parallel p} t_0$ or $\xi^q d\omega_{\perp q} t_0$ a distance R_n away. Adding the vectors $\vec{R}_n - \vec{R}_{a\parallel}$ and $\vec{R}_{a\parallel} - \vec{R}_a$ and taking the modulus with the aid of the above two equations gives us

$$|\vec{R}_n - \vec{R}_a| = \xi^p t_0 R_n d\omega_{\parallel p} \quad \text{if } p > q, \quad (80)$$

$$= \xi^p t_0 R_n \left(d\omega_{\parallel p}^2 + d\omega_{\perp p}^2 \right)^{1/2} \quad \text{if } p = q, \quad (81)$$

which finally leads to

$$\log \left(\frac{|\vec{R}_n - \vec{R}_a|}{t_0 R_n} \right) = p \log \xi + \text{constant}. \quad (82)$$

In Eq. (81), use has been made of Pythagoras theorem since $\vec{R}_n - \vec{R}_{a\parallel}$ is perpendicular to $\vec{R}_{a\parallel} - \vec{R}_a$, $\vec{R}_n - \vec{R}_a$ forms the hypotenuse. Eq. (82) is the key to testing the PN accuracy of our analytical solutions against the numerical one. It says that a linear fit between the two logarithms has a slope equal to the integer p . From Eqs. (76) and (77), we know that p is also the PN order at which our analytical solution starts to diverge from the numerical one, if one focuses their attention on the frequencies associated with the dephasings. In our numerical experiments with a handful of cases, we find $p = 2 \pm 2.5\%$, which indicates that the analytical solutions (both kinds) deviate from the numerical one at 2PN order, as far as the combined (in-plane and out-of-plane) dephasing effect goes. To compute the PN parameter ξ , we use the orbit-averaged value of R , i.e. $\xi = GM/(c^2 \langle R \rangle)$.

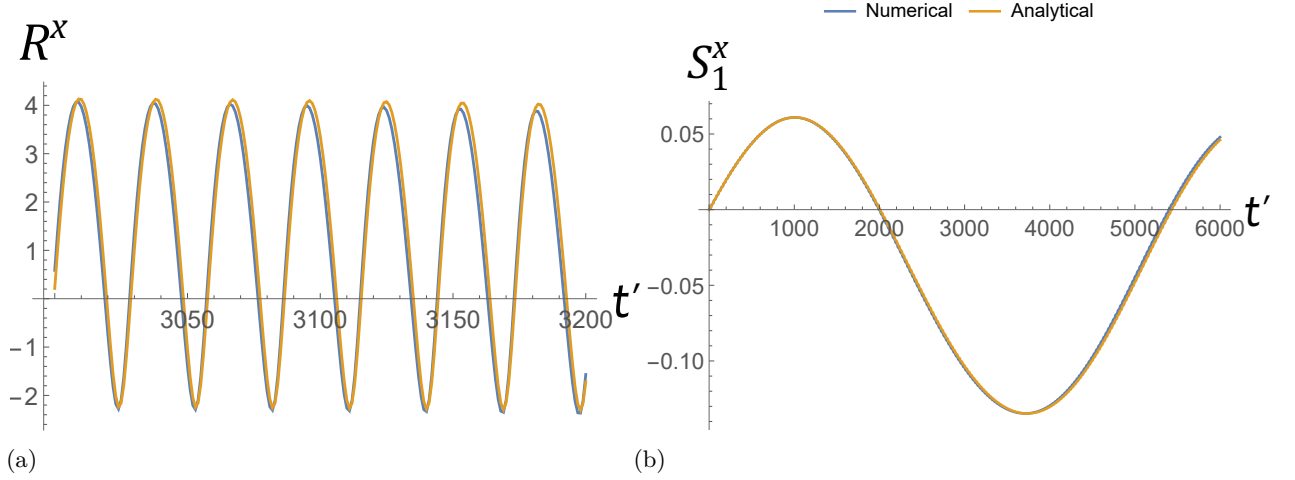


FIG. 2: Comparison of the analytical solutions with the numerical one. For a system with $(m_1, m_2) = (5/2, 1)$ and the initial values of the phase-space variables being $\vec{R} = (2, 2, 2)$, $\vec{P} = (1/2, -1/2, 1/3)$, $\vec{S}_1 = \sqrt{\epsilon} (0, 1, 1)$, $\vec{S}_2 = \sqrt{\epsilon} (1, -3/10, 0)$. Subfigures (a) and (b) show evolution of x -component of \vec{R} and \vec{S}_1 , respectively. We choose $\epsilon = 0.003$ for (a) and $\epsilon = 0.01$ for (b). All this results in a Newtonian-orbital time period of $T_N \sim 29$ for both (a) and (b), and the PN parameter ~ 0.0036 for (a) ~ 0.012 for (b) respectively. Throughout we keep $G = 1$.

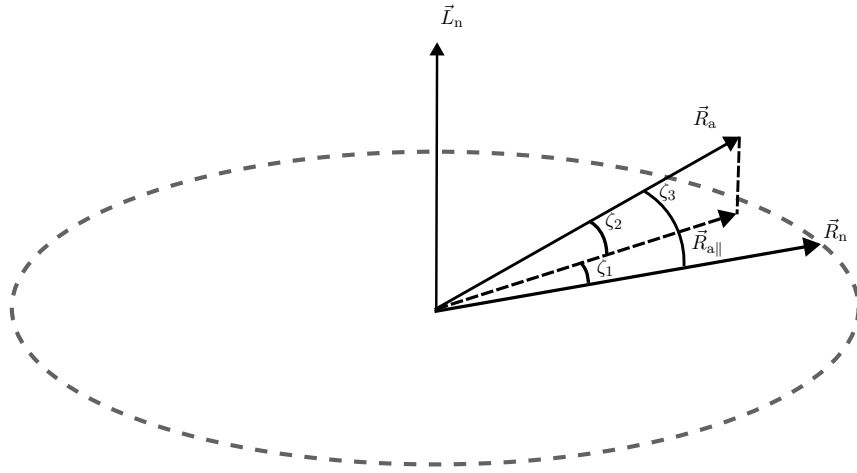


FIG. 3: Difference between the numerical and analytical position vector \vec{R} being split in two perpendicular components.

Another way to compare the analytical solutions with the numerical one is to compare the timescale T_N of variation of the Newtonian orbit against timescale T_D at which $\vec{R}_n - \vec{R}_a$ varies. Assuming a relation of the form

$$T_N = \xi^p T_D, \quad (83)$$

our objective is to determine p . The above equation gives

$$\log T_D = -p \log \xi + \log T_N, \quad (84)$$

A linear fit between the two logarithms in the above equation gives us a slope which is equal to $-p$. We can

approximate T_D as

$$T_D = \frac{2\pi t_1}{\arccos \hat{R}_n \cdot \hat{R}_a}, \quad (85)$$

and ξ is to be approximated the same way as before. This linear fit gave as $-p = -2 \pm 2.5\%$, which again means that the analytical and the numerical solutions differ at 2PN order. We finally mention that the verification of the solutions presented here also serves as a verification for the five action variables constructed in Refs. [18, 19].

There is a subtle aspect of the above procedure of determining the PN accuracy of the analytical solutions which needs further elaboration. A natural question arises: how to vary the PN parameter $\xi \equiv GM/(c^2 R)$? Let's

put forth two options: (1) vary the average value of R (physically sensible) (2) vary $\epsilon = 1/c^2$ (unphysical). We will argue below that the latter option, though unphysical, is the mathematically sound option and the former is not.

The multiplicative factors attached to powers of ξ in Eqs. (76) and (77) are assumed to depend on quantities like energy, mass ratio etc. This comes from our previous experience of the PN literature; for example see the expression of the mean motion in Eq. (49) or Eq. (28-b) of Ref. [28]. So, this means that care must be taken while selecting the sample BBH systems for performing the above linear fits so that all the systems which are supposed to fall on a straight line have almost the same energy and mass ratio. This can be achieved by varying c , while keeping other parameters like m_1, m_2 and average R the same. Doing so does vary ξ . Varying the masses or the average R does change the PN parameter ξ , but also changes the energy and the mass-ratio in general, which is something we want to avoid. The unphysical aspect of varying the speed of light is of no concern to us because our mathematical solutions to the BBH system are valid for any arbitrary positive speeds of light, provided $\xi \rightarrow 0$.

VI. SUMMARY

With this paper, we conclude the old problem of solving the dynamics of the 1.5PN BBH system, whose Hamiltonian was introduced in Ref. [7]. This is done for arbitrary masses, spins and eccentricity, and without any averaging. First we re-presented the solution of Ref. [22] but for completeness, unlike Ref. [22], we included the 1PN effects too. Then we show the reader how to construct the alternative AA-based solution in an algorithmic style. The construction of the latter solution requires inputs from the former. But the AA-based solution is superior in the sense that it can be extended to 2PN order via canonical perturbation theory, with relative ease. We finally introduce `BBHpnToolkit`, a MATHEMATICA package which implements our solutions for practical use. We finally make comparison of the two analytical solutions against the numerical one.

The theoretical ideas that form the foundations of the two analytical solutions have been presented in Refs. [18, 19, 22]; here we have assembled them, filled in the gaps (missing 1PN effects in Ref. [22]), implemented the solutions in a public MATHEMATICA package, thereby establishing a platform (both in theoretical and practical-implementation sense) from where we can aim to push these solutions to 2PN. Moreover, the agreement between the numerical and AA-based solution serves as a non-trivial check of all the five actions constructed in Refs. [18, 19].

The next natural line of action would be to extend our AA-based solution to 2PN order using canonical perturbation theory. On a parallel track, one can try to construct GWs for these systems now that their dynamics have been solved. Adding the 2.5PN dissipative effects due to

radiation reaction to our analytic solution will also be an interesting endeavor for the future.

ACKNOWLEDGMENTS

S.T. thanks Nicolás Yunes for an invitation to conduct a lecture workshop at the University of Illinois Urbana-Champaign. The workshop served as the initial impetus for this project. We also thank Nathan Johnson-McDaniel for providing useful suggestions, and José T. Gálvez Gherzi for a careful reading of this manuscript. The work of L.C.S. was partially supported by NSF CAREER Award PHY-2047382.

Appendix A: Solution for flow under commuting constants

1. Solution for flow under H

The solution of flow under H has been constructed in Sec. III. It is mainly contained in Eqs. (12), (32), (39), (45), (70), and (74).

2. Solution for flow under $S_{\text{eff}} \cdot L$

The solution of flow under $S_{\text{eff}} \cdot L$ has been constructed in Ref. [19]; it is mainly contained in Eqs. (65), (89), (99) and (120). These four equations don't seem to determine \vec{S}_2 and \vec{P} . But once we have \vec{R} , \vec{L} , and \vec{S}_1 , determining \vec{S}_2 and \vec{P} is quite easy. The former is found via $\vec{S}_2 = \vec{J} - \vec{L} - \vec{S}_1$, and the latter is determined using following facts (i) under the $S_{\text{eff}} \cdot L$ flow, P is a constant (ii) $\vec{L} = \vec{R} \times \vec{P}$; hence \vec{L} is perpendicular to \vec{R} and \vec{P} . (iii) under the $S_{\text{eff}} \cdot L$ flow, the azimuthal angle of \vec{P} (around \vec{L}) changes by the same amount as that of \vec{R} . Note that the definitions and conventions of Ref. [19] don't totally align with those followed in this paper; so care has to be taken when merging the results of the two papers.

3. Solution for flow under J

As arrived at in Sec. VI-B of Ref. [19], the effect of a flow under J by an amount $\Delta\lambda$ is increasing the azimuthal angles of \vec{R} , \vec{P} , \vec{S}_1 , and \vec{S}_2 in IF by an amount $\Delta\lambda$.

4. Solution for flow under L

As also arrived at in Sec. VI-B of Ref. [19], the effect of a flow under L by an amount $\Delta\lambda$ is increasing the azimuthal angles of \vec{R} , and \vec{P} in NIF by an amount $\Delta\lambda$.

5. Solution for flow under J_z

As seen in Sec. VI-B of Ref. [19], the effect of a flow under J_z by an amount $\Delta\lambda$ is increasing the azimuthal angles of \vec{R} , \vec{P} , \vec{S}_1 , and \vec{S}_2 by an amount $\Delta\lambda$, around the z -axis of the the inertial frame.

Appendix B: The BBHpnToolkit package

Here we give the details on some coded expressions in our `BBHpnToolkit` package containing unnecessary higher PN order terms. Doing so does not increase the actual PN accuracy of our solutions since we never make use of the 2PN terms of the Hamiltonian. However doing so may bring the analytical solutions closer to the numerical solution (got by numerically integrating the 1.5PN EOMs)

- As mentioned already at the end of Sec. III D, we have kept more than necessary PN accuracy in Eq. (68) and by extension, Eq. (70). All the terms containing ϵ^q with $q \geq 2$ in Eq. (68) are unnecessary.
- The derivation of the solution Eqs. (12)-(28) of the mutual angles between the angular momenta for a flow under the Hamiltonian depends on the integration $\int dt/r^3$; see Eq. (3.6) of Ref. [17]. Here Newtonian r is enough for the desired level of accuracy, and Eqs. (12)-(28) have been derived using Newtonian r in $\int dt/r^3$. But in our `BBHpnToolkit`, we have coded the results got by integrating 1.5PN accurate $1/r^3$. Eqs. (46) give the 1.5PN r .

-
- [1] B. Abbott *et al.* (LIGO Scientific, Virgo), GWTC-1: A Gravitational-Wave Transient Catalog of Compact Binary Mergers Observed by LIGO and Virgo during the First and Second Observing Runs, *Phys. Rev. X* **9**, 031040 (2019), arXiv:1811.12907 [astro-ph.HE].
- [2] R. Abbott *et al.* (LIGO Scientific, Virgo), GWTC-2: Compact Binary Coalescences Observed by LIGO and Virgo During the First Half of the Third Observing Run, (2020), arXiv:2010.14527 [gr-qc].
- [3] B. P. Abbott *et al.* (LIGO Scientific, Virgo), GW170817: Observation of Gravitational Waves from a Binary Neutron Star Inspiral, *Phys. Rev. Lett.* **119**, 161101 (2017), arXiv:1710.05832 [gr-qc].
- [4] L. Blanchet, Gravitational Radiation from Post-Newtonian Sources and Inspiralling Compact Binaries, *Living Rev. Rel.* **17**, 2 (2014), arXiv:1310.1528 [gr-qc].
- [5] G. Schäfer and P. Jaranowski, Hamiltonian formulation of general relativity and post-Newtonian dynamics of compact binaries, *Living Rev. Rel.* **21**, 7 (2018), arXiv:1805.07240 [gr-qc].
- [6] T. Damour and N. Deruelle, General relativistic celestial mechanics of binary systems. I. The post-Newtonian motion., *Ann. Inst. Henri Poincaré Phys. Théor* **43**, 107 (1985).
- [7] B. M. Barker, S. N. Gupta, and R. D. Haracz, One-Graviton Exchange Interaction of Elementary Particles, *Phys. Rev.* **149**, 1027 (1966).
- [8] S. Tiwari, A. Gopakumar, M. Haney, and P. Hemandakumar, Ready-to-use Fourier domain templates for compact binaries inspiraling along moderately eccentric orbits, *Phys. Rev. D* **99**, 124008 (2019), arXiv:1905.07956 [gr-qc].
- [9] M. Kesden, D. Gerosa, R. O’Shaughnessy, E. Berti, and U. Sperhake, Effective Potentials and Morphological Transitions for Binary Black Hole Spin Precession, *Phys. Rev. Lett.* **114**, 081103 (2015), arXiv:1411.0674 [gr-qc].
- [10] D. Gerosa, M. Kesden, U. Sperhake, E. Berti, and R. O’Shaughnessy, Multi-timescale analysis of phase transitions in precessing black-hole binaries, *Phys. Rev. D* **92**, 064016 (2015), arXiv:1506.03492 [gr-qc].
- [11] I. Hinder, L. E. Kidder, and H. P. Pfeiffer, Eccentric binary black hole inspiral-merger-ringdown gravitational waveform model from numerical relativity and post-Newtonian theory, *Phys. Rev. D* **98**, 044015 (2018), arXiv:1709.02007 [gr-qc].
- [12] K. Chatziioannou, A. Klein, N. Yunes, and N. Cornish, Constructing gravitational waves from generic spin-precessing compact binary inspirals, *Phys. Rev. D* **95**, 104004 (2017), arXiv:1703.03967 [gr-qc].
- [13] A. Klein and P. Jetzer, Spin effects in the phasing of gravitational waves from binaries on eccentric orbits, *Phys. Rev. D* **81**, 124001 (2010), arXiv:1005.2046 [gr-qc].
- [14] A. Klein, Y. Boetzel, A. Gopakumar, P. Jetzer, and L. de Vittori, Fourier domain gravitational waveforms for precessing eccentric binaries, *Phys. Rev. D* **98**, 104043 (2018), arXiv:1801.08542 [gr-qc].
- [15] C. Konigsdorffer and A. Gopakumar, Phasing of gravitational waves from inspiralling eccentric binaries at the third-and-a-half post-Newtonian order, *Phys. Rev. D* **73**, 124012 (2006), arXiv:gr-qc/0603056.
- [16] C. Konigsdorffer and A. Gopakumar, Post-Newtonian accurate parametric solution to the dynamics of spinning compact binaries in eccentric orbits: The Leading order spin-orbit interaction, *Phys. Rev. D* **71**, 024039 (2005), arXiv:gr-qc/0501011.
- [17] G. Cho and H. M. Lee, Analytic Keplerian-type parametrization for general spinning compact binaries with leading order spin-orbit interactions, *Phys. Rev. D* **100**, 044046 (2019), arXiv:1908.02927 [gr-qc].
- [18] S. Tanay, L. C. Stein, and J. T. Gálvez Ghersi, Integrability of eccentric, spinning black hole binaries up to second post-Newtonian order, *Phys. Rev. D* **103**, 064066 (2021), arXiv:2012.06586 [gr-qc].
- [19] S. Tanay, G. Cho, and L. C. Stein, Action-angle variables of a binary black-hole with arbitrary eccentricity, spins, and masses at 1.5 post-Newtonian order, (2021), arXiv:2110.15351 [gr-qc].
- [20] S. Tanay, Integrability and action-angle-based solution of the post-Newtonian BBH system (lecture notes) (2022) arXiv:2206.05799 [gr-qc].

- [21] <https://github.com/sashwattanay/BBH-PN-Toolkit> (2022).
- [22] G. Cho and H. M. Lee, Analytic Keplerian-type parametrization for general spinning compact binaries with leading order spin-orbit interactions, *Phys. Rev. D* **100**, 044046 (2019), [arXiv:1908.02927 \[gr-qc\]](https://arxiv.org/abs/1908.02927).
- [23] A. Fasano, S. Marmi, and B. Pelloni, *Analytical Mechanics: An Introduction*, Oxford Graduate Texts (OUP Oxford, 2006).
- [24] V. Arnold, K. Vogtmann, and A. Weinstein, *Mathematical Methods of Classical Mechanics*, Graduate Texts in Mathematics (Springer New York, 2013).
- [25] J. José and E. Saletan, *Classical Dynamics: A Contemporary Approach* (Cambridge University Press, 1998).
- [26] A. Gopakumar and G. Schafer, Gravitational wave phasing for spinning compact binaries in inspiraling eccentric orbits, *Phys. Rev. D* **84**, 124007 (2011).
- [27] H. Goldstein, C. Poole, and J. Safko, *Classical Mechanics* (Pearson, 2013).
- [28] G. Cho, S. Tanay, A. Gopakumar, and H. M. Lee, Generalized quasi-Keplerian solution for eccentric, non-spinning compact binaries at 4PN order and the associated IMR waveform, (2021), [arXiv:2110.09608 \[gr-qc\]](https://arxiv.org/abs/2110.09608).